

This item was submitted to Loughborough's Institutional Repository (<https://dspace.lboro.ac.uk/>) by the author and is made available under the following Creative Commons Licence conditions.



CC creative commons
COMMONS DEED

Attribution-NonCommercial-NoDerivs 2.5

You are free:

- to copy, distribute, display, and perform the work

Under the following conditions:

 **Attribution.** You must attribute the work in the manner specified by the author or licensor.

 **Noncommercial.** You may not use this work for commercial purposes.

 **No Derivative Works.** You may not alter, transform, or build upon this work.

- For any reuse or distribution, you must make clear to others the license terms of this work.
- Any of these conditions can be waived if you get permission from the copyright holder.

Your fair use and other rights are in no way affected by the above.

This is a human-readable summary of the [Legal Code \(the full license\)](#).

[Disclaimer](#) 

For the full text of this licence, please go to:
<http://creativecommons.org/licenses/by-nc-nd/2.5/>

31st August 2004
revised

Electrochemical Reactivity of TiO₂ Nanoparticles Adsorbed onto Boron- Doped Diamond Surfaces

Frank Marken*¹, Avninder S. Bhambra¹, Duk-Hyun Kim²,
Roger J. Mortimer¹, Susan J. Stott¹

¹ *Department of Chemistry, Loughborough University, Loughborough,
Leicestershire LE11 3TU, UK.*

² *Dept. of Bio- and Chemical Engineering, Korea Polytechnic University, 3Ga-101,
Jungwang-Dong, Shihung-City, Kyonggi-Do, 429-450, Korea.*

To be submitted to *Electrochemistry Communications*

Proofs to F. Marken

Email: F.Marken@lboro.ac.uk

Abstract

TiO₂ (anatase) nanoparticles of ca. 6-10 nm diameter are adsorbed from acidic aqueous solution onto polycrystalline industrially polished boron-doped diamond electrode surfaces. After immobilisation at the electrode surface, TiO₂ nanoparticles are imaged in vacuum by electron microscopy (FEGSEM) and when immersed in a liquid film of aqueous 12 M LiCl by in situ scanning tunnelling microscopy (STM). Mono-layer films of TiO₂ particles are studied voltammetrically in different electrolyte media.

Boron-doped diamond as an inert substrate material allows the reduction of TiO₂ particles in phosphate buffer solution to be studied and two distinct steps in the reduction - protonation process are identified: (i) a broad reduction signal associated with the binding of an outer layer of protons and (ii) a sharper second reduction signal associated with the binding of an inner (or deeper) layer of protons. Voltammetric experiments in aqueous 0.1 M NaClO₄ with variable amounts of HClO₄ suggest that the reduction of TiO₂ particles is consistent with the formation of Ti(III) surface sites and accompanied by the adsorption of protons. Saturation occurs and the total amount of surface sites can be determined. Preliminary data for electron transfer processes at the reduced TiO₂ surface such as the dihydrogen evolution process and the 2 electron - 2 proton reduction of maleic acid to succinic acid are discussed.

Keywords: TiO₂, anatase, nanoparticle, assembly, adsorption, boron-doped diamond, surface electrochemistry, voltammetry, hydrogen evolution, electrocatalysis.

1. Introduction

Titanium dioxide, TiO_2 , is a versatile material with a wide range of uses for pigment [1] to photocatalyst [2] and to dimensionally stable electrode [3] applications. The surface chemistry has been carefully studied at polycrystalline and at single crystal surfaces [4]. TiO_2 has been studied extensively usually in the form of thin meso- or microporous films at inert electrodes [5], at titanium surfaces [6,7,8], but also in the form of single crystals [9,10].

The electrochemical properties of mesoporous films of TiO_2 have been intensely studied [11,12,13,14] and recently models have been developed [15] to describe the capacitive and reactive properties of nanoporous semiconducting TiO_2 . However, relatively little is known about the behaviour of individual TiO_2 nanoparticles or ensembles of TiO_2 nanoparticles assembled into a mono-layer. It is shown here that electrochemical experiments with mono-layer deposits of TiO_2 can be readily conducted and provide data complementary to results from thick film and single crystal experiments. When immobilized into a mono-layer of nanoparticles, TiO_2 shows features similar to those of polyoxometalate redox systems [16] with surface site reduction (here Ti(IV/III)) and protonation. Experiments were conducted at boron-doped diamond substrates.

Boron-doped diamond [17] as an inert electrode material has found a wide range of applications in electroanalysis [18], electrosynthesis [19], and waste treatment [20]. The chemically inert diamond surface combined with a wide accessible potential window and low background current make boron-doped diamond an ideal substrate

material for the immobilisation of sensor probes [21] and for the study of materials which are otherwise not or only very difficult to study. Various types of nanoparticles (gold [22,23], platinum [24] and other metals [25], hydrous iron oxide [26], ruthenium oxide [27], and iridium oxide [28]) have previously been immobilised at boron-doped diamond surfaces and investigated with voltammetric techniques.

In this preliminary report, experiments are described in which titanium dioxide, TiO₂ (anatase), nanoparticles are adsorbed onto the surface of a polycrystalline boron-doped diamond electrode (industrially polished to mirror finish) and studied in aqueous solution environments. STM imaging demonstrates the presence of a homogeneous film deposit and the reduction response for the TiO₂ nanoparticles is proposed to be associated with the formation of surface Ti(III) and accompanied by the adsorption of protons. Two distinct types of sites for the reduction process associated with proton adsorption are observed.

2. Experimental

2.1. Chemical Reagents

LiCl, phytic acid (*myo*-inositol hexakis(dihydrogen phosphate) dodecasodium salt), maleic acid, NaClO₄, HClO₄ (70% in water), K₂HPO₄, KH₂PO₄, were obtained commercially (Aldrich) and used without further purification. Demineralised and filtered water was taken from an Elga water purification system (Elga, High Wycombe, Bucks) with a resistivity of not less than 18 MOhm cm. Titania (anatase) sol (30-35 % in aqueous HNO₃, pH 0 to 1, TKS-202) was obtained from Tayca Corp., Osaka, Japan, and diluted tenfold with water prior to use.

2.2. Instrumentation

Electrochemical experiments were conducted with a PGSTAT 30 Autolab system (Eco Chemie, Netherlands) in a 50 mL three-electrode cell. The counter electrode was a platinum gauze, the reference electrode was a saturated Calomel electrode (SCE, Radiometer). Polycrystalline boron-doped diamond with mirror-finish polish (mineral acid treated, doping level ca. 10^{21} cm^{-3} , Windsor Scientific, Slough, UK) was obtained in the form of plates (5 mm \times 5 mm \times 0.6 mm) for electrochemical experiments (mounted with silver epoxy back contact in epoxy) and in the form of 3 mm diameter disks (for STM and FEGSEM experiments). The aqueous solution was thoroughly de-aerated with argon (BOC) prior to conducting experiments. Experiments were conducted at $22 \pm 2 \text{ }^\circ\text{C}$.

For Field Emission Gun Scanning Electron Microscopy (FEGSEM) a Leo 1530 system was used. Samples were prepared by scratching and gold sputter coating prior to analysis. Scanning tunnelling microscopy images were obtained with a Nanosurf EasyScan System (Windsor Scientific, Slough, UK) with a Pt-Ir tip and conventional scan settings (512 points per line, 10 Hz). For good images to be obtained, the sample was covered with a thin film of aqueous ca. 12 M LiCl (equilibrated in air).

3. Results and Discussion

3.1. Adsorption of TiO₂ Nanoparticles onto Boron-Doped Diamond Surfaces

Boron-doped diamond surfaces after treatment with mineral acids have oxygen functionalised surfaces and allow some types of positively charged colloids to readily adsorb. It has been shown recently that boron-doped diamond allows nanoparticulate

oxides such as hydrous iron oxide [26] and ruthenium oxide [27], to be adsorbed onto the surface in the form of a very thin layer. This configuration with an inert and geometrically well-defined boron-doped diamond surface substrate (see Scheme 1) allows the electrochemical properties of the nanoparticle deposits to be studied and potential distribution effects within the oxide layer or within the pores of the oxide to be minimised.

Figure 1 shows a FEGSEM image of a boron-doped diamond surface modified with a layer of TiO₂ nanoparticles adsorbed onto the electrode surface from an aqueous 3% solution. The diamond is flat and featureless and the TiO₂ nanoparticles appear in the form of aggregates of 10 – 40 nm diameter. In the lower part of the micrograph, the particles have been removed by scratching with a scalpel blade. The presence of the homogeneous nanoparticle layer is confirmed by in situ liquid environment (aqueous ca. 12 M LiCl) STM imaging (see Figure 2). A clean boron-doped diamond surface appears to have a roughness of less than 1 nm peak-to-peak. After adsorption of the TiO₂ nanoparticles, the film deposit can be clearly seen again with aggregates of typically 10-40 nm diameter.

3.2. Surface Electrochemistry of TiO₂ Nanoparticles at Boron-doped Diamond

Electrode Surfaces

The voltammetric response from a polished boron-doped diamond electrode immersed in aqueous 0.1 M phosphate buffer at pH 7 between +0.5 V vs. SCE and – 1.8 V vs. SCE is featureless and consistent with a clean background (not shown). After adsorption of a TiO₂ monolayer a new reduction response is detected commencing at a potential of –0.8 V vs. SCE. The shape of this voltammetric

response (see Figure 3Ai) is characteristic for TiO₂ thin films and has been explained in terms of sequential filling electronic states within the oxide [15]. For TiO₂ films more extended than a mono-layer, this voltammetric response is dominating the overall behaviour. However, for the mono-layer deposit new features can be observed.

Scanning the potential more negative allows a new peak feature to be observed, which is less broad than the first reduction signal. After reversal of the scan direction (see Figure 3Aii) two peak features are observed also during oxidation. Scanning the potential further into the negative potential range causes the oxidation peak to shift positively and a shoulder towards even more positive potentials develops. It is likely that the shift in the oxidation peak potential is associated with a change in the proton binding at the TiO₂ surface.

In order to explore the involvement of protons in the TiO₂ reduction and re-oxidation processes, voltammetric experiments were conducted in unbuffered aqueous 0.1 M NaClO₄ with small concentrations of protons. Under these conditions a similar set of voltammetric responses is observed (see Figure 3B) and the two reduction peaks are again observed. Both, the first and the second reduction signal are highly symmetric (consistent with the presence of reversible surface states) and only when the potential is scanned into more negative potentials, a shift of the oxidation peak occurs (probably associated with a gradual structural re-arrangement at the surface). Perhaps surprisingly, reducing the concentration of protons from 1 mM to 0.5 mM and finally to 0.1 mM (see Figures 3B, C, and D, respectively) causes the second reduction peak to disappear and the first reduction peak to become smaller. This behaviour is consistent with a proton depletion effect within the aqueous solution phase and proves

the direct involvement of protons in the reduction process. The Randles Sevcik equation [29] (equation 1) allows the current peak for mass transport controlled depletion of protons to be calculated.

$$I_p = -0.446 n F A c \sqrt{\frac{nFvD}{RT}} \quad (1)$$

In this equation the peak current for the reduction, I_p , is expressed in terms of $n=1$, the number of electrons transferred per proton, F , the Faraday constant, $A=2.5 \times 10^{-5} \text{ m}^2$, the geometric electrode area, $v=0.1 \text{ Vs}^{-1}$, the scan rate, $D=1 \times 10^{-8} \text{ m}^2\text{s}^{-1}$, the approximate diffusion coefficient for protons, R , the gas constant, and T , the absolute temperature. The calculated peak current for a proton concentration of 0.1 mM is $I_p=21 \times 10^{-6} \text{ A}$ consistent with the voltammetric results (see Figure 3D). Therefore, proton adsorption occurs and the two reduction peaks may be attributed to two distinct binding sites for protons in the vicinity of Ti(III) sites. A schematic drawing (see Scheme 2) is illustrating this situation. The total number of binding sites can be estimated from the charge under the voltammetric response as ca. 150 μC for both H_a and H_b . Taking into account the amount of TiO_2 particles on the boron-doped diamond surface (see Figure 1, ca. 10^{12} particles on $5 \text{ mm} \times 5 \text{ mm}$) this suggests ca. 1000 electrons per 6 nm diameter TiO_2 particle, consistent with a surface process (there are approximately 3300 Ti atoms per 6 nm diameter anatase particle).

It is interesting to explore the kinetic effects coupled to proton binding at the TiO_2 surface. At a sufficiently slow scan rate, the reduction process becomes chemically irreversible (see Figure 3D) and proton reduction to dihydrogen has been suggested in

the literature [30,31]. The oxidation response is diminished at a scan rate of approximately $v_{\text{transition}} = 0.5 \text{ V s}^{-1}$ and the rate constant for the surface process can be estimated as $k = \frac{A_{\text{total}} F v_{\text{transition}}}{RT} = 2 \times 10^{-3} \text{ m}^2 \text{ s}^{-1}$ (with $A_{\text{total}} \approx 10^{-4} \text{ m}^2$). However, in the presence of a higher concentration of protons, when the second reduction process occurs, the voltammetric response becomes more reversible and the dihydrogen evolution process is apparently suppressed. The peak-shape of the second reduction process suggests a process ‘deeper’ within the surface (see H_b) and it may be speculated that this will reduce the availability of electrons for the two-electron reduction of protons to dihydrogen at sites denoted H_a (see Scheme 2). One possible implication of this observation is that small quantities of fully reduced TiO₂ nanoparticles will behave chemically different when compared to thicker layer of mesoporous TiO₂.

3.3. Electron Transfer Processes at TiO₂ Nanoparticles Adsorped onto Boron-Doped Diamond Electrode Surfaces

The availability of electrons within the TiO₂ particles and the availability of binding sites at the TiO₂ surface poses the question whether selective reduction processes can be driven electrochemically at the TiO₂ surface in the presence of the inert boron-doped diamond electrode surface. Electrochemical reduction processes at TiO₂ electrodes have been well studied [32] and it has recently been reported that olefins with carboxylate group, such as maleic acid [33], can be reduced electrocatalytically at TiO₂ electrodes. This report is confirmed here for the case of a single layer of TiO₂ nanoparticles.

Figure 3E shows the effect of adding maleic acid (ca. 1 mM) into an aqueous solution of 0.1 NaClO₄ and 1 mM HClO₄. A new chemically irreversible reduction response is observed at -0.8 V vs. SCE consistent with the potential for the first reduction of the TiO₂ surface. This process is not observed at a polished boron-doped diamond electrode (not shown and therefore entirely due to the presence of TiO₂ as 'electrocatalyst'. The peak current, $I_p = 130 \mu\text{A}$ (see Figure 3E), is consistent with a 2 electron 2 proton reduction of maleic acid to succinic acid (using equation 1). Finally, addition of a competitive binder, here phytic acid (see Figure 3Eii), reduces the current for the electrocatalytic reduction process and possibly introduces a novel way of controlling reactivity and selectivity at the TiO₂ surface.

There are several beneficial features of employing mono-layers or well-defined amounts of titanium dioxide electrocatalyst nanoparticles immobilised at boron-doped diamond electrodes. With thick film TiO₂ electrodes, dihydrogen evolution can occur in competition to other beneficial reduction processes, but at thin film TiO₂ electrodes and at sufficiently negative potentials, the suppression of the competing dihydrogen evolution process appears to be possible. A catalytic reduction process may be optimised by judicious choice of proton concentration, olefin concentration, catalyst amount, and applied potential. In future, the presence of a co-binder at the TiO₂ surface may be employed to control the selectivity of the reduction process or to introduce chirality. However, more experimental work will be required to further improve the fundamental knowledge on electrochemical TiO₂ surface processes.

4. Conclusions

It has been shown that voltammetric experiments with mono-layer films of TiO₂ (anatase) nanoparticles at boron-doped diamond electrodes surfaces give insights into oxide surface processes, the type and availability of binding sites, and the reactivity and the mechanism of surface processes. Boron-doped diamond is a versatile and highly beneficial substrate material and there may be real benefits (in terms of efficiency and selectivity of electron transfer processes) in employing very thin films of nanoparticles on boron-doped diamond substrates. In situ STM imaging in an aqueous environment has been demonstrated and this technique could in future yield much more detailed in situ information about the surface processes. More experimental work for example with more uniform TiO₂ materials will be required to improve the fundamental understanding of surface electrochemical processes at TiO₂ surfaces and at similar oxide electrode surfaces.

Acknowledgements

F.M. thanks the Royal Society for the award of a University Research Fellowship. S.J.S. thanks the RSC and the EPSRC for an Analytical Science Studentship. Tayca Corporation is gratefully acknowledged for donating titania sols.

Captions to Figures

Scheme 1

Schematic drawing of an active nanoparticle deposit immobilised at an inert boron-doped diamond electrode surface.

Scheme 2

Schematic drawing of the TiO₂ surface with binding sites for protons (A) and for maleic acid (B).

Figure 1

FEGSEM image of a deposit of TiO₂ nanoparticles (agglomerates of 10-40 nm diameter) on a boron-doped diamond substrate.

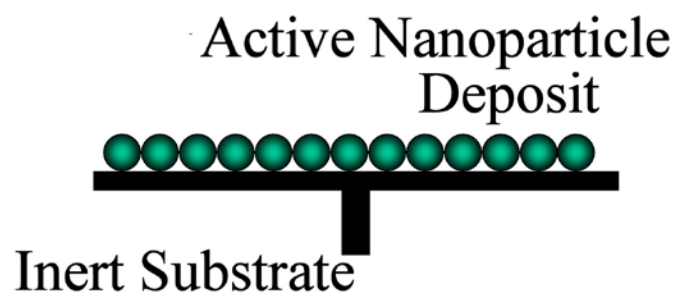
Figure 2

STM images of (A) a clean boron-doped diamond surface and (B) after deposition of TiO₂ nanoparticles. Images were obtained in the presence of aqueous 12 M LiCl to improve conductivity.

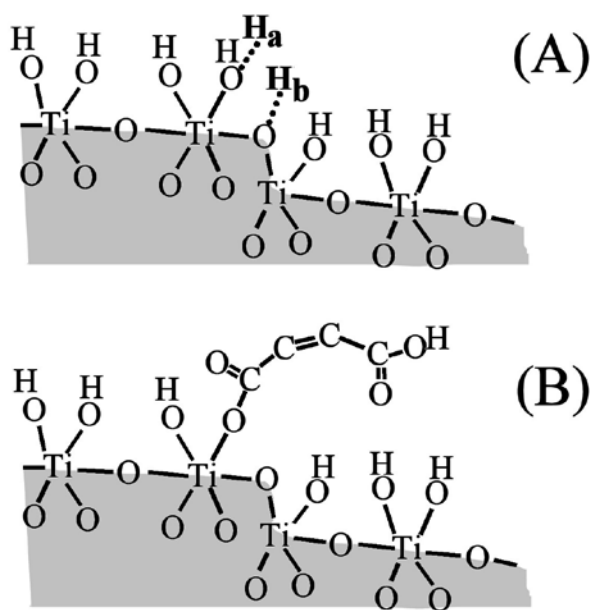
Figure 3

Cyclic voltammograms obtained for the reduction of a mono-layer deposit of TiO₂ nanoparticles at a 5 mm × 5 mm boron-doped diamond plate electrode (A) immersed in aqueous 0.1 M phosphate buffer pH 7 with variable reversal potential (scan rate 100 mV s⁻¹), (B) immersed in aqueous 0.1 M NaClO₄/ 1 mM HClO₄ with variable reversal potential (scan rate 100 mV s⁻¹), (C) immersed in aqueous 0.1 M NaClO₄/ 0.5 mM HClO₄ with variable scan rate of (i) 100, (ii) 200, (iii) 500, (iv) 1000 mV s⁻¹, (D)

immersed in aqueous 0.1 M NaClO₄/ 0.1 mM HClO₄ with variable scan rate of (i) 100, (ii) 200, (iii) 500, (iv) 1000 mV s⁻¹, and (E) immersed in aqueous 0.1 M NaClO₄/ 1 mM HClO₄ (i) with 1 mM maleic acid and in (ii) with 1 mM phytic acid added (scan rate 100 mV s⁻¹).



Scheme 1



Scheme 2

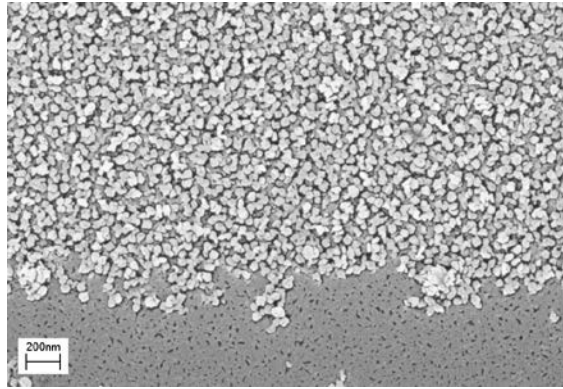


Figure 1

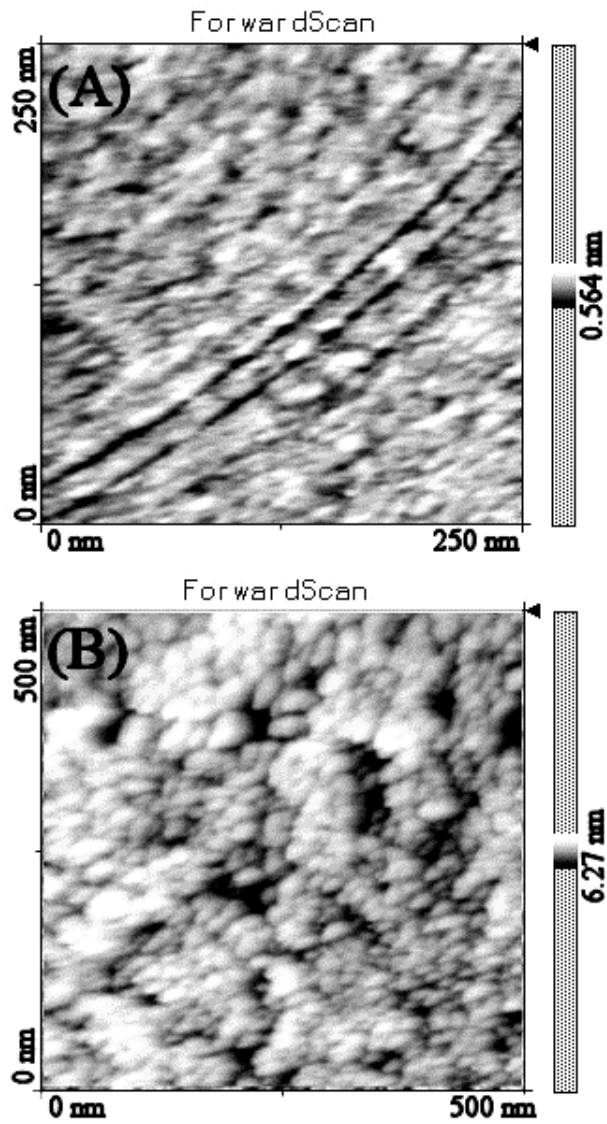


Figure 2

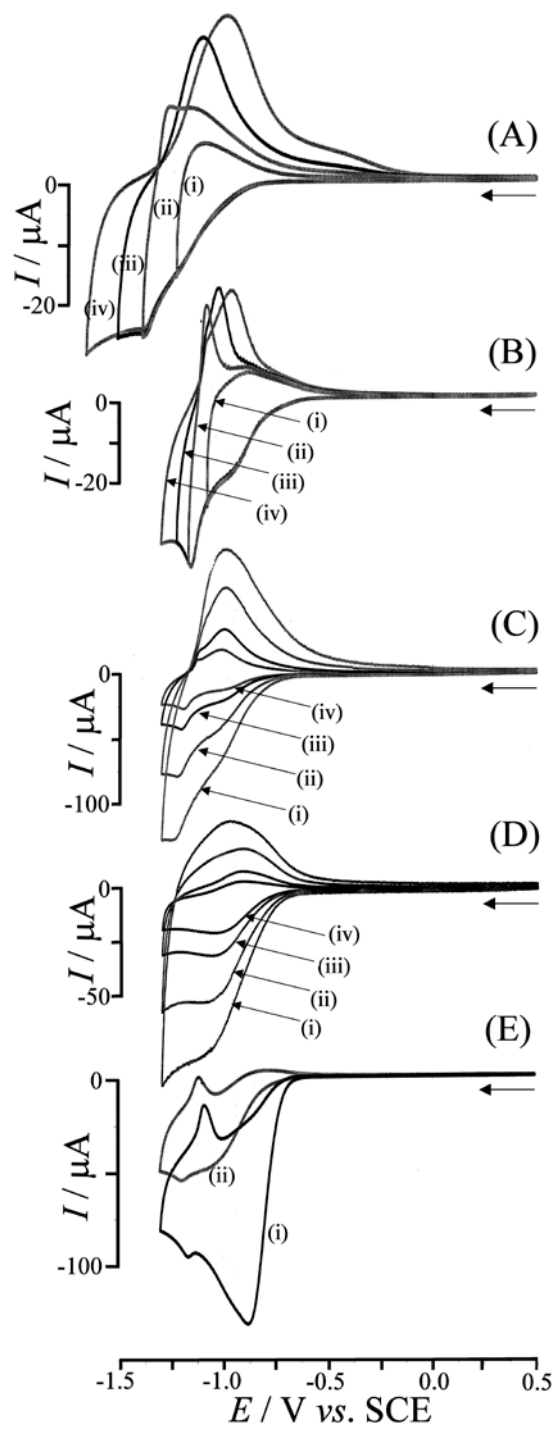


Figure 3

References

- 1 See for example C.S. Fang, Y.W. Chen, *Mater. Chem. Phys.* 78 (2003) 739.
- 2 See for example A. Fujishima, K. Hashimoto, T. Watanabe, *TiO₂ Photocatalysis Fundamentals and Applications*, BKC Inc., Tokyo, 1997.
- 3 See for example H. Wendt, G. Kreysa, *Electrochemical Engineering*, Springer, Berlin, 1999.
- 4 For a review see U. Diebold, *Surf. Sci. Rep.* 48 (2003) 53.
- 5 See for example I. Abayev, A. Zaban, F. Fabregat-Santiago, J. Bisquert, *Phys. Stat. Sol. A-Appl. Res.* 196 (2003) R4.
- 6 C.J. Boxley, H.S. White, C.E. Gardner, J.V. Macpherson, *J. Phys. Chem. B* 107 (2003) 9677.
- 7 See for example E.M. Oliveira, C.E.B. Marino, S.R. Biaggio, R.C. Rocha-Filho, *Electrochem. Commun.* 2 (2000) 254.
- 8 see for example O.R. Camara, C.P. De Pauli, M.C. Giordano, *Electrochim. Acta* 29 (1984) 1111.
- 9 See for example H. Pelouchova, P. Janda, J. Weber, L. Kavan, *J. Electroanal. Chem.* 566 (2004) 73.
- 10 R. Memming, *Semiconductor Electrochemistry*, Wiley-VCH, Weinheim, 2001.
- 11 see for example L. Kavan, M. Gratzel, J. Rathousky, A. Zukal, *J. Electrochem. Soc.* 143 (1996) 394.
- 12 G. Boschloo, D. Fitzmaurice, *J. Electrochem. Soc.* 147 (2000) 1117.
- 13 J. Bisquert, *J. Phys. Chem. B* 108 (2004) 2323.
- 14 I. Mora-Sero, J. Bisquert, *Nano Lett.* 3 (2003) 945.

-
- 15 F. Fabregat-Santiago, I. Mora-Sero, G. Garcia-Belmonte, J. Bisquert, *J. Phys. Chem. B* 107 (2003) 758.
- 16 See for example T. Yamase, M.T. Pope, *Polyoxometalate Chemistry for Nano-composite Design*, Kluwer Academic, Amsterdam, 2003.
- 17 Yu. V. Pleskov, *Russ. J. Electrochem.* 38 (2002) 1275.
- 18 R.G. Compton, J.S. Foord, F. Marken, *Electroanalysis* 15 (2003) 1349.
- 19 See for example J.D. Wadhawan, F.J. Del Campo, R.G. Compton, J.S. Foord, F. Marken, S.D. Bull, S.G. Davies, D.J. Walton, S. Ryley, *J. Electroanal. Chem.* 507 (2001) 135.
- 20 L. Ouattara, M.M. Chowdhry, C. Comninellis, *New Diam. Front. Carb. Technol.* 14 (2004) 239.
- 21 See for example L. Su, X.P. Qiu, L.H. Guo, F.H. Zhang, C.H. Tung *Sens. Actuators B-Chem.* 99 (2004) 499.
- 22 Y.R. Zhang, S. Asahina, S. Yoshihara, T. Shirakashi, *Electrochim. Acta* 48 (2003) 741.
- 23 K.B. Holt, G. Sabin, R.G. Compton, J.S. Foord, F. Marken, *Electroanalysis* 14 (2002) 797.
- 24 F. Montilla, E. Morallon, I. Duo, C. Comninellis, J.L. Vazquez, *Electrochim. Acta* 48 (2003) 3891.
- 25 J.S. Gao, T. Arunagiri, J.J. Chen, P. Goodwill, O. Chyan, J. Perez, D. Golden *Chem. Mater.* 12 (2000) 3495.
- 26 K.J. McKenzie, D. Asogan, F. Marken, *Electrochem. Commun.* 4 (2002) 820.
- 27 K.J. McKenzie, F. Marken, *Electrochem. Solid State Lett.* 5 (2002) E47.
- 28 C. Terashima, T.N. Rao, B.V. Sarada, N. Spataru, A. Fujishima, *J. Electroanal. Chem.* 544 (2003) 65.

-
- 29 See for example F. Scholz (ed.), *Electroanalytical Methods*, Springer, Berlin, 2002, p.64.
- 30 See for example Y. Doi, M. Tamaki, *Inorg. Chim. Acta* 64 (1982) L145 and references cited therein.
- 31 M. Ashokkumar, *Int. J. Hydrogen Energy* 23 (1998) 427.
- 32 See for example V.B. Baez, J.E. Graves, D. Pletcher, *J. Electroanal. Chem.* 340 (1992) 273.
- 33 J.S. Gu, D.B. Chu, X.F. Zhou, G.X. Shen *Acta Chim. Sin.* 61 (2003) 1405.